J. Phys. Chem. A **2001,** *105,* 6841−6850

Hydrogen-Bonded Bridges in Complexes of *o*-Cyanophenol: Laser-Induced Fluorescence and IR/UV Double-Resonance Studies

M. Broquier, F. Lahmani,* and A. Zehnacker-Rentien†

Laboratoire de Photophysique Moléculaire du CNRS, Bât. 210, Université de Paris XI, 91405 Orsay Cédex, France

V. Brenner and Ph. Millié

CEA-Saclay, Service des Photons, Atomes et Molécules, Laboratoire Francis Perrin, Bât 522, 91191 Gif-sur-Yvette Cedex, France

A. Peremans

Facultés Universitaires Notre-Dame de la Paix Physics Department, LASMOS Laboratory, 61 rue de Bruxelles, B-5000 Namur, Belgique

Received: January 19, 2001; In Final Form: April 13, 2001

The *o*-cyanophenol molecule and its hydrogen-bonded complexes with one and two molecules of water and methanol have been investigated by laser-induced fluorescence excitation, dispersed emission, and IR/UV double-resonance spectroscopy combined with DFT calculations. The sole conformer observed in the jet has a cis geometry due to the stabilizing interaction between the OH and CN substituents. The shifts of the electronic transition and the modification of the OH ground-state frequencies together with the calculated geometry point to a cyclic structure of the complexes. In the 1:1 complexes, the solvent OH binds as a proton acceptor to the phenol OH and as a proton donor to the CN group. The 1:2 complexes involve in a similar way the insertion of the solvent dimer (water)$_2$ or (methanol)$_2$ between the OH and CN substituents of the molecule.

Introduction

Aromatic molecules bearing an acidic proton such as phenol and 1- or 2-naphthol undergo a strong enhancement of their acidity in the excited state and provide thus ideal systems for examining fundamental aspects of photoinduced proton-transfer reactions. While the photophysics of the hydrogen-bonded complexes involving the generic phenol and naphthol molecules and various bases have been widely investigated in gas-phase clusters,[1] much less attention has been paid to the properties of their derivatives.

The effect of introducing a substituent on hydroxyaromatic compounds is two-fold. First, depending on the electron-donating or -accepting character of the substituent, it can modify the acidity of the chromophore. For example, it has been found that the presence of a methoxy group in the para position from the phenolic OH group in salicylic acid prevents the intramolecular photoinduced proton-transfer reaction.[2] On the other hand, phenol derivatives bearing an electron-withdrawing group such as cyano, NO_2, or sulfonate are known to exhibit an enhanced acidity[3,4] in both the ground and excited states, which in turn is expected to facilitate the excited-state proton transfer.

Second, the dissymmetry introduced by a substituent located ortho or meta from the hydroxy group of phenol results in the existence of two isomers, namely cis and trans, which correspond to two different orientations of the OH group relative to the second substituent. When the substituent acts as a proton acceptor site, a stabilizing intramolecular interaction (weak hydrogen bond) takes place in the cis conformer. The relative stability of the cis and trans conformers depends thus on the strength of the internal H bond. Cis and trans isomers, which show different intersystem crossing efficiencies, have been postulated for the *o*-chlorophenol molecule.[5] On the other hand, only one isomer has been evidenced in jet-cooled *o*-fluorophenol[6] and catechol,[7] as shown by hole burning together with high-resolution electronic spectroscopy.[6] The formation of an internal H bond results in a decrease of the force constant and thus a red shift of the frequency of the OH stretching mode, as shown by Fujii et al. in the case of *o*-fluorophenol.[8] In the presence of water or other proton-accepting solvents, the balance between the intermolecular H bonds and the internal H bond may influence the conformation[9,10] of such bifunctional compounds.

In this work we have investigated the electronic and vibrational spectroscopy of jet-cooled *o*-cyanophenol, denoted hereafter *o*-CNPhOH, and its clusters with water or methanol using laser-induced fluorescence and double-resonance UV/IR techniques. Our choice was guided by the following criteria extracted from literature data: the ground-state gas-phase acidity is larger by 16.2 kcal/mol than that of phenol.[11] In solution, the pK_a is strongly decreased in the singlet excited state of all the cyano derivatives of phenol. It is the smallest for the ortho derivative (0.66), and both the neutral and anion fluorescence have been observed.[12] Moreover, the *o*-cyanophenol molecule may present two isomers corresponding to the cis or trans orientation of the OH group with respect to the neighboring CN group. The cis form with the OH hydrogen pointing toward the CN substituent is expected to be stabilized by a weak

---

† E-mail: anne.zehnacker@ppm.u-psud.fr.

10.1021/jp010218n CCC: $20.00

intramolecular hydrogen bond but both cis and trans forms have been evidenced in infrared spectra of *o*-cyanophenol solutions at room temperature.[13] Finally, the interaction of protic solvents with both the donor (OH) and the accepting (CN) sites of the *o*-cyanophenol chromophore may result in different types of hydrogen-bonded structures, whose nature (linear or cyclic) is determined by the balance between the intermolecular and intramolecular forces.

The technique of IR/UV dip spectroscopy recently developed provides a well-adapted tool to probe the ground-state OH stretch frequencies in isolated H-bonded molecules and complexes and to characterize the binding sites in such systems.[14] To deduce structural information from the experimental results, density functional theory (DFT) has been used to calculate the geometry of the complexes and the corresponding harmonic vibrational frequencies.

I. Methods

A. Experimental Details. The setup used for excitation and dispersed emission experiments has been described previously and rests on the laser-induced fluorescence detection of van der Waals complexes formed in a continuous supersonic expansion of helium (2−3 atm). The molecules are excited in the cold region of the jet by means of a frequency-doubled dye laser (DCM) pumped by the second harmonic of a YAG laser (BM Industrie or Quantel). The fluorescence is observed at a right angle through a WG335 cutoff filter by a Hamamatsu R2059 photomultiplier. The signal is monitored by a Lecroy 9400 oscilloscope connected to a PC computer.

The setup used for the IR/UV double-resonance experiments combines a pulsed jet (General Valve) and two 20 Hz OPO lasers (BBO for the visible one, and $LiNbO_3$ for the infrared one). The OPO system consists of an original prototype first developed at the Centre Laser Infrarouge d'Orsay (CLIO) and rests on two OPO synchronously pumped by a pulsed mode-locked Nd:YAG laser.[15] The YAG oscillator is fitted with an intracavity nonlinear absorber in order to generate trains (macropulses) of 50 micropulses at a repetition rate of 20 Hz. The micropulse duration and separation are 12 ps and 10 ns, respectively.

The use of two YAG laser heads, one for the oscillator and one for the amplification, enables us to provide up to 1.1 W of pump power at 1064 nm. One-third of the pump power, 350 mW, is used to synchronously pump a $LiNbO_3$-based OPO, while the remaining pump power, 750 mW, is frequency tripled to generated 200 mW of pump beam at 355 nm for the BBO-based OPO. Both UV and IR OPO lasers possess the same temporal structure as the YAG laser. The bandwidths of the signal beams oscillating in the OPO cavities are constrained by Etalon plates in order to obtain nearly Fourier transform-limited tunable picosecond micropulses. The idler beam of the $LiNbO_3$/OPO is tunable from 2.6 to 4 μm and has a bandwidth of 3 cm^{-1} (FWMH) at 3 μm and a micropulse duration of 10 ps. Its power at 3 μm is 25 mW. The signal beam of the visible OPO is tunable from 410 to 700 nm and has a bandwidth of 3 cm^{-1} at 550 nm and a micropulse duration of 9 ps. Its power is maintained at 12 mW.

The IR spectra are recorded with the fluorescence dip IR spectroscopy technique, a variant of the double-resonance technique first introduced by Lee[16] and co-workers. This technique, pioneered by Riehn et al.,[17] Tanabe et al.,[18] and Pribble et al.[19] is a powerful means to obtain detailed infrared spectra of jet-cooled clusters. In this experiment, the recorded fluorescence signal is averaged over the whole macropulse. The short lifetime of the S_1 state together with the peculiar temporal characteristics of the laser make the absorption from the S_1 state very unlikely in our experimental conditions.

B. Theoretical Details. Theoretical calculations have been performed to determine the most stable structure of the different complexes and to assign the vibrational frequencies observed in the UV and IR spectra.

We have combined first a model potential with a global optimization method to explore the intermolecular potential surface. Then a local optimization with the DFT calculation, by means of the Gaussian 98 software package,[20] has been performed to determine the fully-optimized geometry and the harmonic vibrational frequencies. For the DFT method we have used the combined Becke's three-parameter exchange functional and the gradient-corrected functional of Lee, Yang, and Parr (B3LYP functional).[21]

(1) Semiempirical Method. To extensively explore the whole potential energy surface, we have used a model for the description of the intermolecular interaction, and a global optimization method to find the minima, in which the intramolecular geometries are kept frozen. This strategy enables us to determine the equilibrium structures and the different contributions to the interaction energy. This method initially developed by Claverie et al.[22] is based on the exchange perturbation theory and has already been successfully applied to van der Waals complexes.[23] The interaction energy as already described[24] is obtained as a sum of four terms: electrostatic, polarization, dispersion, and short-range repulsion. To evaluate the electrostatic term, a simplified multipolar distribution (a charge, a dipole, and the quadrupole on each atom and bond center) has been generated for each molecule from the multicenter multipolar development, which derives from the correlated wave function within the cc-pvTZ basis set. The polarization term is based on the same multipole expansion as above, plus experimental atom and bond polarizabilities. The dispersion and repulsion contributions were expressed as a sum of atom−atom terms. An extension of the simulated annealing method[25] has been used for the localization of the minima. First, a random search on the surface is performed by the Metropolis algorithm[26] in order to determine the different attraction basins of the potential energy surface. Second, the conformations obtained from this exploration are sorted out. Finally, the resulting conformations are optimized by a local minimization method,[27] which leads to the determination of the most stable isomers. It has been shown[28] that the minima generated by the model potential are very close to the minima obtained with a quantum chemistry method. These geometries have therefore been used as starting points for the local optimization by means of DFT methods.

(2) DFT Calculations. Previous theoretical work[29] has been done at the RHF level for the geometry optimization of the orthocyanophenol molecule, using the standard cc-pvDZ basis set. In our case, the geometry optimization and the harmonic vibrational frequencies calculation of the parent monomers and the complexes were done at the B3LYP level of theory using the standard cc-pvTZ basis set.[30]

In such calculations, the basis set superposition error (BSSE) that arises from the use of finite atomic basis sets needs to be considered. Even if this error may be estimated by the counterpoise method of Boys and Bernardi,[31] its dependence upon the intermolecular coordinates cannot be easily evaluated.[32] The use of the large cc-pvTZ basis set results in the minimization of the BSSE contribution. Moreover this basis set possesses sufficient angular flexibility to properly represent the polariza-

TABLE 1: Comparison of Experimental Observed Vibrational Frequencies of *o*-Cyanophenol with Calculated Ones (Frequencies in cm^{-1})

ν_{EXP} S_1	ν_{EXP} S_0	ν_{CAL}	assignments[a]	assignments[b]
129	116	138	in-plane substituent bending	
129	130[c]	133	out-of-plane antisym butterfly OH−N	
180	275	?		
258 = 2 × 129				
370	367	391	C−OH bending	
442	455	475	δ(CC), ν(CC), δ(C−O)	6_a
498 = 370 + 129				
568 = 442 + 129				
669	582	613	CH + OH−CN bending	
813	836	862	ν(CC), δ(CC), δ(CO)	12
	906 = 455 × 2			
940	1016	1054	ν(CC), δ(CH)	18a
		1247		9_b
	1241	1281	ν(CO), ν(CC), δ(CH)	X-sensitive
	1289	1338	ν(CO), ν(CC), δ(CH)	X-sensitive
	3586	3746	ν(OH)	

[a] Qualitative normal modes decomposition. [b] Associated normal modes of benzene derivatives. [c] From 0−0 + 129 cm^{-1} excitation (see text).

tion. As no contribution of dispersion is included in the DFT method, the use of aug-cc-pvTZ basis set with diffuse atomic orbitals is not necessary.

To assess the validity of the calculated geometries and binding energies obtained at the B3LYP/cc-pvTZ level, we have compared them to those obtained at the MP2/cc-pvTZ level in the case of the *o*-CNPhOH−H_2O complex. Both methods yield substantially the same geometry (the intermolecular coordinates are the same within less than 1% for both distances and angles while the intramolecular coordinates are even closer to each other) and the same interaction energies.

Using the geometry optimized at the B3LYP/cc-pvTZ level, the computed interaction energies are the same for both B3LYP/cc-pvTZ and MP2/cc-pvTZ (denoted MP2//B3LYP) methods (see Table 3). Therefore, the use of the MP2 level of theory, which would require very long calculation times, is not necessary and the DFT method is fully justified for the systems presented here.

Owing to the large anharmonicity of the OH stretch and the fact that the BSSE correction can vary along the coordinate describing the vibrational motion, the calculated OH frequency (see Table 4) is, as usually observed,[33] overestimated relative to the experimentally observed value. This systematic error has not been corrected by a scaling factor, since this factor can be different for modes of different anharmonicity. Instead of that, we have chosen to compare for each complex under study the experimental shift of the vibrational transition relative to the bare molecule with the calculated one. The anharmonicity of the phenolic OH stretch has been evaluated by calculating the effect of deuteration on the shift induced by complexation with H_2O and CH_3OH. For both complexes, the overestimation due to anharmonicity is about 30% of the calculated frequency shift.

II. Results

A. S_0−S_1 LIF Spectra of *o*-Cyanophenol and Its Clusters. *(1) Bare Molecule.* The fluorescence excitation spectrum of *o*-CNPhOH in the region of its origin is shown in Figure 1. The 0−0 transition is located at 33 967 cm^{-1} (294.40 nm compared to 298 nm in nonpolar solvents) and is strongly red-shifted relative to unsubstituted phenol (36 348.7 cm^{-1}) and benzonitrile (36 514 cm^{-1}). A similar shift is observed in solution.[29]

The main vibronic bands observed within ~1000 cm^{-1} above the origin are collected in Table 1. Besides vibrational modes in the region of benzene ring deformations above 372 cm^{-1}, this spectrum clearly shows a low-frequency progression involving a 129 cm^{-1} mode, which also appears in combination

TABLE 2: Overview of Structural Parameters of *o*-Cyanophenol Associated Complexes Calculated at the B3LYP Level Using the CC-PVTZ Basis Set (Distances in Å, Angles in Degrees)[a]

		o-CNPhOH−			
	o-CNPhOH	H_2O	CH_3OH	$(H_2O)_2$	$(CH_3OH)_2$
Distances					
$r(O_5{-}H_6)$	0.97	0.99	0.99	0.99	0.99
$r(N_4{-}C_3)$	1.15	1.15	1.15	1.15	1.15
$r(O_7{-}H_8)$		0.97	0.97	0.98	0.98
$r(O_9{-}H_{10})$				0.97	0.97
$R(N_4...H_8)$		2.10	2.10		
$R(O_7...H_6)$		1.77	1.73	1.71	1.68
$R(O_5...O_7)$		2.73	2.71	2.65	2.63
$R(O_7...N_4)$		2.92	2.91		
$R(O_7...O_9)$				2.75	2.75
$R(O_9...N_4)$				2.83	2.82
$R(N_4...H_{10})$				1.93	1.92
Angles					
$\theta(C_2{-}C_3{-}N_4)$	176.0	178.4	178.5	178.9	178.4
$\theta(C_1{-}O_5{-}H_6)$	110.5	116.5	116.6	118.1	118.2
$\theta(O_5{-}H_6{-}O_7)$		166.3	166.2	156.1	156.8
$\theta(O_7{-}H_8{-}N_4)$		140.7	139.6		
$\theta(O_9{-}H_{10}{-}N_4)$				152.3	153.4
$\theta(O_7{-}H_8{-}O_9)$				173.5	168.9
Dihedral Angles					
$\omega(C_2{-}C_1{-}O_5{-}H_6)$	0.0	0.2	2.2	−1.0	5.3
$\omega(C_1\text{-}C_2{-}C_3{-}N_4)$	0.0	−7.0	−5.5	168.2	169.1
$\omega(C_1{-}O_5{-}H_6...O_7)$		175.0	164.8	178.5	162.0
$\omega(C_2{-}C_3{-}N_4...H_8)$		7.5	3.3		
$\omega(C_2{-}C_3{-}N_4...H_{10})$				−172.8	−172.6

[a] For atom numbering see Figures 7 and 8.

TABLE 3: Results of the Standard B3LYP/cc-pVTZ Calculation on the Different *o*-Cyanophenol Complexes (Energies in kcal/mol)

	o-CNPhOH−			
	H_2O	CH_3OH	$(H_2O)_2$	$(CH_3OH)_2$
E_B[a]	−10.9	−10.8	−22.07	−21.62
ΔE_{BSSE}	2.21	2.03	3.93	3.84
ΔE[b]	−8.66[c]	−8.77	−18.14	−17.78
D_0[d]	−6.54	−7.31	−13.77	−14.92

[a] Binding energy. [b] $\Delta E = E_B + \Delta E_{BSSE}$. [c] At MP2, $\Delta E = -8.72$ kcal/mol; at MP2//B3LYP, $\Delta E = -8.70$ kcal/mol. [d] $D_0 = \Delta E +$ ZPE.

TABLE 4: Comparison between Experimental Vibrational Frequencies and Calculated Vibrational Harmonic Frequencies (Frequencies in cm^{-1}, Calculated Infrared Intensities in km/mol)

	ν(OH phenolic)			ν(OH donor to C≡N)			ν(OH free)			ν(OH solvent dimer)		
	exp	cal	int	exp	cal	int	exp	cal	int	exp	cal	int
o-CNPhOH	3586	3747	82									
o-CNPhOH−H_2O	3322	3373	968	3595	3707	148	3731	3864	104			
	$\Delta\nu$	$\Delta\nu$										
	264	374										
o-CNPhOH−CH_3OH	3165	3309	1229	3591	3720	218						
	$\Delta\nu$	$\Delta\nu$										
	421	438										
o-CNPhOH-$(H_2O)_2$	3202	3270	1372	3518	3609	682	3722	3864/3867	64/103	3427[a]	3453	460
	$\Delta\nu$	$\Delta\nu$										
	384	477										
o-CNPhOH-$(CH_3OH)_2$	3085	3207[b]/3204[b]	1131/444	3505	3618	852				3322[c]	3472	642
	$\Delta\nu$	$\Delta\nu$										
	501	540										
o-CNPhOH−H_2O) ("open form")		3544	978					3794[d]/3891[e]	19/87			

[a] $(H_2O)_2$: 3601 cm^{-1}. [b] Coupled with the streching CH. [c] $(CH_3OH)_2$: 3574 cm^{-1}. [d] Correlated to water ν_1 mode. [e] Correlated to water ν_3 mode.

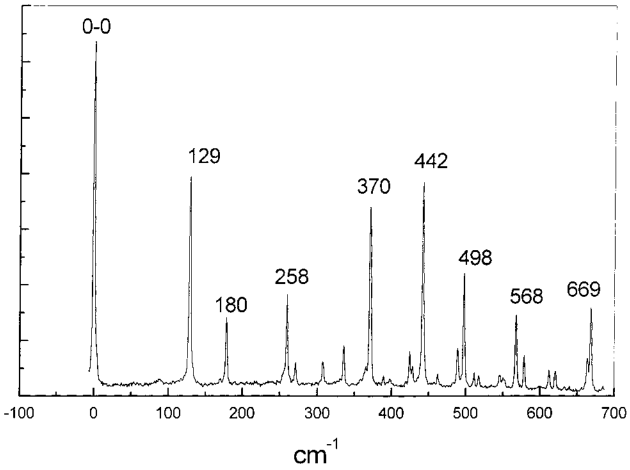

Figure 1. Fluorescence excitation spectrum of jet-cooled *o*-cyanophenol. The 0−0 transition is at 33 967 cm^{-1}.

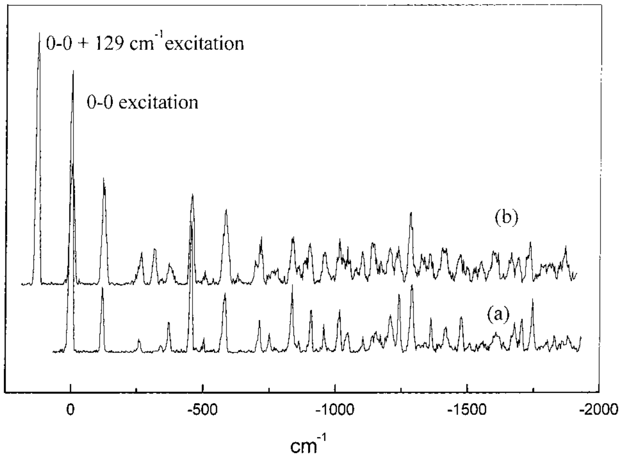

Figure 2. Dispersed fluorescence emission spectra of *o*-cyanophenol (a) excited to the S_1 origin at 33 967 cm^{-1} and (b) excited to the 0−0 + 129 cm^{-1} level. The frequency scale is relative to the electronic origin.

with the most intense bands in the excitation spectrum, and a weaker band at 180 cm^{-1}. These vibrations indicate the presence of large amplitude motions located on the substituents.

The dispersed emission spectrum obtained by pumping the v = 0 and 129 cm^{-1} levels is shown in Figure 2, and the ground-state vibrational frequencies obtained from fluorescence spectra of selected vibronic levels are also listed in Table 1. A low-frequency mode of 117 cm^{-1} shows up in the emission, resulting from the excitation of the origin band. It can be assigned to the ground-state counterpart of the S_1 129 cm^{-1} mode. The emission spectrum resulting from the excitation of the 129 cm^{-1} mode displays a $\Delta v = 0$ band, which is broader than the experimental resolution and peaks at 130 cm^{-1} from the excitation. It can be assigned to the overlap of two unresolved bands, one of them being the 1−1 transition at 117 cm^{-1}, the other one corresponding to the 1−1 transition of another mode. This behavior denotes the mixing of vibrational states due to the rotation of the normal modes upon excitation (Duchinsky effect[34]). This anomaly in the emission spectra occurs when the geometry of the excited state differs from that of the ground state. Furthermore, the broad Franck−Condon envelop of the emission extending over more than 3000 cm^{-1} indicates a significant deformation of the molecule between ground and excited states.

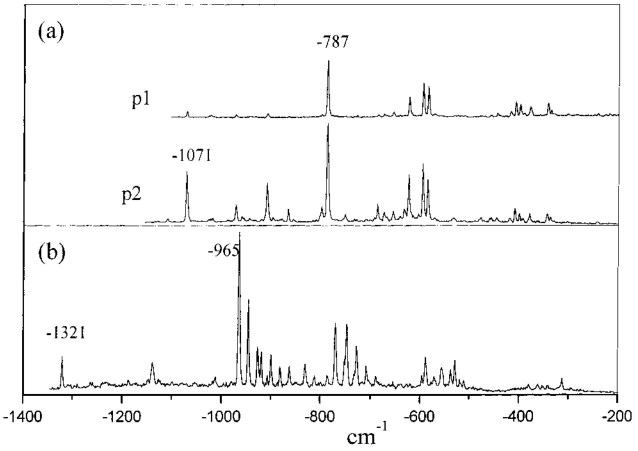

Figure 3. Fluorescence excitation spectrum of *o*-cyanophenol (a) in the presence of H_2O at two different partial pressures (p2 = 2p1) (b) in the presence of methanol. The energy scale is relative to the bare molecule origin.

The main features observed in both excitation and emission can be analyzed in terms of a single species and fail to reveal the presence of a second isomer. This result is confirmed by the UV/IR double-resonance experiment, as described below.

(2) Water Complexes. Figure 3a shows the fluorescence excitation spectrum obtained by adding different amounts of water to *o*-CNPhOH. The linear intensity dependence on the water partial pressure of the most intense feature appearing at

-787 cm^{-1} from the origin of the bare molecule shows that it can be assigned to the 0−0 transition of the 1:1 complex. By increasing the water vapor pressure, new bands appear further to the red, with the most shifted band located at -1071 cm^{-1} from the bare molecule origin. The quadratic intensity dependence of the band located at -1071 cm^{-1} on the water partial pressure shows that it is due to the 1:2 complex. The excitation spectrum obtained by detecting the fluorescence in the red part of the spectrum at $\lambda > 375$ nm where the cyanophenolate anion is expected to emit gives no evidence of the excited proton-transfer reaction even with helium saturated with water vapor pressure at room temperature ($p = 25$ Torr).

Complexation with one water molecule induces a strong modification of the low-frequency pattern of the *o*-CNPhOH chromophore since the intense 129 cm^{-1} mode observed in the bare molecule cannot be clearly identified in the excitation spectrum. Instead, three prominent features that can be assigned to intermolecular modes appear at 162, 191, and 201 cm^{-1} from the 0−0 transition of the 1:1 complex. This result indicates that the structure of the *o*-cyanophenol chromophore is affected by complexation with one water molecule.

The dispersed fluorescence (not shown) obtained by exciting the 0−0 level of the 1:1 complex is resonant and shows the same typical frequencies due to the substituted benzene ring as observed for uncomplexed *o*-CNPhOH at 455, 836, 1016, and 1289 cm^{-1}. There are, however, some differences in the low-frequency-modes spectral region: The main bands appearing in this region are located at 148 and 185 cm^{-1}. Dispersed fluorescence spectra obtained by exciting the 162, 191, and 201 cm^{-1} features of the 1:1 complex show that their ground-state counterparts are 148, 170, and 185 cm^{-1}, respectively. The increase of these low-frequency modes when going from S_0 to S_1 indicates the stiffening of the hydrogen bonds upon excitation.

The 0−0 transition of the 1:2 complex at -1071 cm^{-1} from the 0−0 transition of the bare molecule is shifted furthermore to the red by 284 cm^{-1} with respect to the 1:1 complex. Its low-frequency vibronic pattern is simpler than in the 1:1 complex: a strong band is found at 161 cm^{-1} and a weak band pops up at 100 cm^{-1} from the origin. The dispersed fluorescence obtained by pumping the 0−0 transition exhibits two bands at 130 and 185 cm^{-1} from the excitation line.

(3) Methanol Complexes. The excitation spectra of the *o*-CNPhOH in the presence of methanol is presented in Figure 3b. Depending on the partial pressure of methanol, two different clusters can be assigned in this spectrum, similarly to the case of water complexes. The most intense feature appearing at -965 cm^{-1} from the origin of the bare molecule is assigned to the 1:1 complex and is followed by a progression built on a 20 cm^{-1} frequency mode. The same progression is observed in combination with two modes observed at 195 and 217 cm^{-1}. The spectrum appearing further to the red exhibits a quadratic dependence upon the methanol partial pressure and is thus assigned to the 1:2 complex. It has its origin located at -1321 cm^{-1} from the bare molecule 0−0 transition and is much less congested than the 1:1 complex. A single intense vibronic band appears at 181 cm^{-1} from the origin.

The dispersed fluorescence obtained by pumping the 0−0 transition of the 1:1 and 1:2 complexes is resonant. The spectrum of both complexes exhibits in the low-frequency region an intense band located at 200 and 164 cm^{-1}, respectively.

B. IR Spectra of *o*-Cyanophenol and Its Complexes in the OH Stretch Region. The infrared-induced fluorescence dip spectrum of the bare *o*-cyanophenol molecule and its complexes with one and two molecules of water and methanol has been investigated in the region of the ν(OH) vibration (3000−4000 cm^{-1} range). The observed frequencies are listed in Table 4. For each complex under study, the number of bands observed in the infrared-induced fluorescence dip spectrum is equal to that of the expected OH oscillators, which confirms the complex stoichiometry.

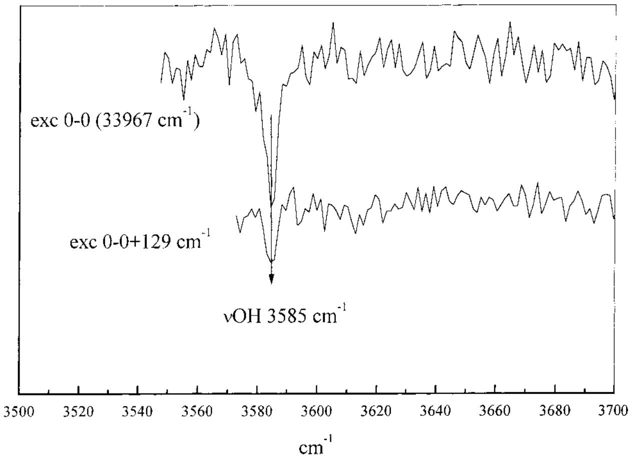

Figure 4. IR/UV double-resonance spectra of bare *o*-cyanophenol probed at the origin of the S_0−S_1 transition and at the 0−0 + 129 cm^{1} level.

(1) Bare Chromophore. When the probe is set on the 0−0 transition of the bare molecule, a single dip appears at 3585 cm^{-1}, as shown in Figure 4. This band can be assigned to the ν(OH) stretching mode of *o*-cyanophenol and is red-shifted by 72 cm^{-1} relative to bare phenol.[14] The band appears at exactly the same frequency with the probe set on the 0−0 + 129 cm^{-1} band. This result shows unambiguously that both excited-state features originate from the same isomer in S_0. The width of the band is about 4−5 cm^{-1}, slightly broader than the laser bandwidth.

(2) Water Complexes. Three bands located at 3322, 3595, and 3731 cm^{-1} respectively are observed in the IR depletion spectrum obtained by setting the probe on the 0−0 transition of the water 1:1 complex, as shown in Figure 5a. These bands differ by their width: while the band located at 3731 cm^{-1} is limited by the experimental resolution, the band located at 3595 cm^{-1} is 4 cm^{-1} broad and the most intense band located at 3322 cm^{-1} is 13 cm^{-1} broad.

The water 1:2 complex IR depletion spectrum is shown in Figure 6a: As observed for the 1:1 complex, a strong band appears below 3 μm. It is located at 3202 cm^{-1} and is 20 cm^{-1} broad. Two other strong bands appear at 3422 and 3518 cm^{-1}, with a similar bandwidth of 12−14 cm^{-1}, together with a narrow band at 3721 cm^{-1} with a laser-limited bandwidth.

(3) Methanol Complexes. When the methanol 1:1 complex 0−0 transition is probed, two bands are observed in the IR depletion spectrum (Figure 5b). The first one is very broad ($\approx$30 cm^{-1}) and located at 3165 cm^{-1}. It is shifted by -419 cm^{-1} from the bare molecule. The other band located at 3590 cm^{-1} is narrow ($\approx$4 cm^{-1}) and intense.

Two strong bands appear in the IR depletion spectrum of the 1:2 complex. Both of them are broader than the laser bandwidth (11 and 7 cm^{-1} for the bands located at 3322 and 3505 cm^{-1}, respectively). A much broader band appears in the red region of the spectrum and extends continuously over more than 120 cm^{-1} up to 3000 cm^{-1} (Figure 6b). We have carefully checked that this broad band arose from the 1:2 complex since no depletion was observed when the probe is set on the fluorescence background due to larger methanol clusters. It is

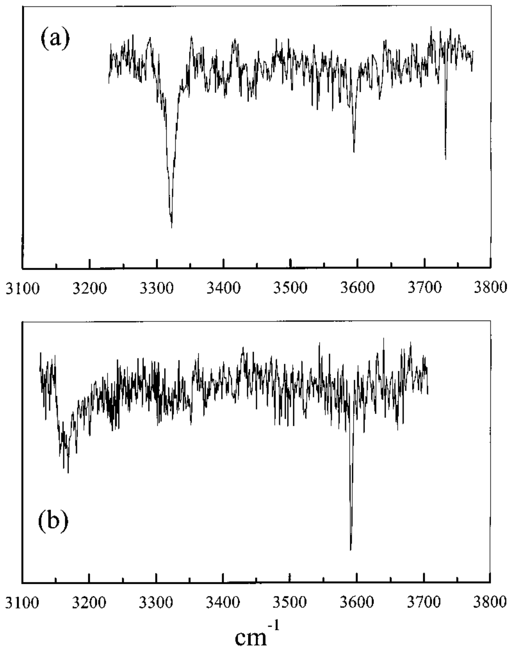

Figure 5. IR/UV double-resonance spectra of (a) *o*-cyanophenol$-H_2O$ 1:1 complex and(b) *o*-cyanophenol$-CH_3OH$ 1:1 complex.

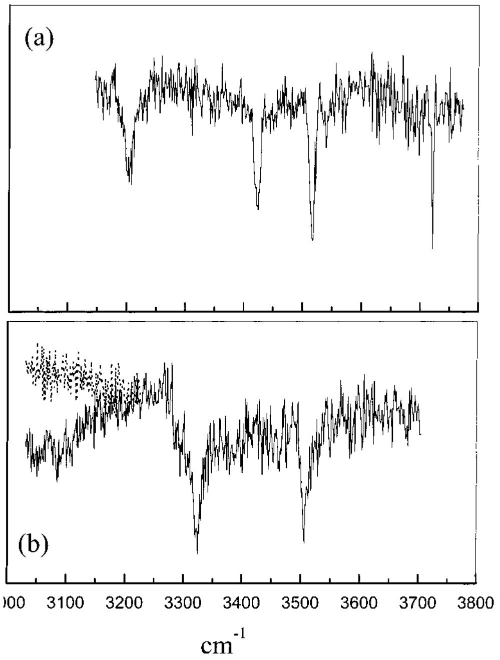

Figure 6. IR/UV double-resonance spectra of (a) *o*-cyanophenol$-H_2O$ 1:2 complex and (b) *o*-cyanophenol$-CH_3OH$ 1:2 complex. The dotted line in Figure 6b corresponds to the reference probe signal (without IR).

also to be noted that no band appears in the blue region of the spectrum where the free OH stretching mode of methanol is expected.

C. Calculations. Several different minima resulting from the global exploration of the potential energy surface have been found. However, the most stable geometry of all four complexes has been unambiguously identified, as their binding energy is at least 2 kcal/mol larger than that of the other isomers.

The most stable structures obtained for the water and methanol complexes are displayed in Figures 7 and 8 and the corresponding structural parameters are listed in Table 2. The atoms of *o*-CNPhOH and the solvents have been labeled according to Figures 7 and 8. The total binding energies of the complexes taking into account the basis set superposition error (BSSE) are reported in Table 3. The calculated harmonic frequencies of the OH stretching modes and the associated intensities are listed in Table 4.

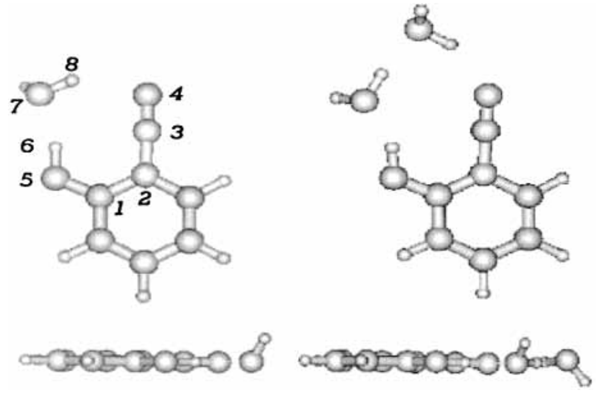

Figure 7. Calculated minimum energy structures of *cis*-*o*-cyanophenol$-H_2O$ (a) 1:1 and (b) 1:2 complexes. The labeling of the atoms is used to define the structural parameters in the text and in Table 4.

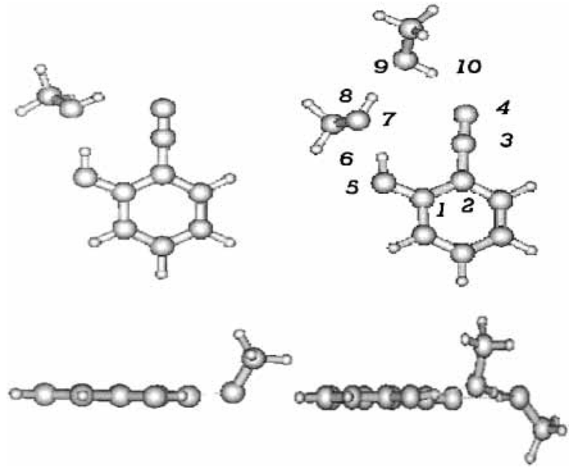

Figure 8. Calculated minimum energy structures of *cis*-*o*-cyanophenol$-CH_3OH$ (a) 1:1 and (b) 1:2 complexes. The labeling of the atoms are used to define the structural parameters in the text and in Table 4.

(1) Bare Chromophore. DFT calculations of the two possible conformers of *o*-cyanophenol have been carried out to provide a basis for assigning the experimentally observed structures. As expected, the cis conformer in which the OH group points toward the CN is found to be more stable than the trans conformer by 2.6 kcal/mol. The OH group is found to lie in the plane of the benzene ring with the $C_1-O_5-H_6$ angle $=$ 110.5° similar to phenol while the $C_2-C_3-N_4$ angle is slightly bent to 176° (Table 2). The calculated harmonic frequencies are listed in Table 1. The calculated difference between the ν(OH) of the cis and the trans form (-68 cm^{-1}) shows that the OH and the CN groups are involved in a weak intramolecular hydrogen bond in the cis conformer.

(2) Water and Methanol Complexes. (a) Geometries. The most stable geometry obtained for the 1:1 water and methanol complexes exhibits a ring structure as shown in Figures 7 and 8. The calculated structures involve the cis form of the chromophore in which the solvent molecule inserts to make a bridge between the OH and the CN substituents. In these structures, the solvent acts as both an H-bond acceptor with respect to the acid phenolic OH and an H-bond donor toward the CN accepting group. However, the solvent molecule lies

closer to the OH group than to the CN group: the calculated O_5-O_7 distances (2.73 and 2.71 Å, respectively, for the 1:1 water and methanol complexes) are much shorter than the calculated O_7-N_4 distances (2.92 and 2.91 Å). The insertion of the solvent molecule modifies the geometry of the *o*-CNPhOH molecule: the $C_1-O_5-H_6$ angle opens up from 110.5° to 116.5° while the $C_2-C_3-N_4$ angle becomes closer to linearity (178.5°) and the CN substituent is slightly bent out of the aromatic plane (7°). In contrast with what is observed in the monohydrated phenol complex,[35,36] one of the water hydrogen atoms lies almost in the plane of the aromatic molecule (the $C_2-C_3-N_4-H_8$ dihedral angle is 3.3° and 7.5° for the water and methanol complexes, respectively). Because of the cyclic structure of the complexes, the $O_5-H_6-O_7$ angle that describes the H bond geometry deviates from linearity by 14°. The main difference between the water and methanol complex lies in a small deviation from planarity: while the O_7 atom of water is about 5° above the molecular plane, the corresponding O_7 atom of methanol is out of the molecular plane by 15°.

The calculated 1:2 water complex exhibits also a cyclic structure in which the water dimer inserts between the OH and CN substituents (Figure 7). In this cluster the hydrogen bonds are also almost coplanar with the phenyl nucleus but not of equal length (the O_5-O_7, O_7-O_9, and O_9-N_4 distances are 2.65, 2.75, and 2.83 Å, respectively). It is to be stressed that the H bond involving *o*-CNPhOH is shorter than in the 1:1 complex (by about 0.08−0.1 Å) and that the intra water dimer H-bond undergoes a shortening of 0.2 Å relative to the free dimer[37] (Table 2). Because of the strain imposed by the water-dimer bridge, the angle $O_5-H_6-O_7$ of the donating OH_{phenol} and the accepting water-dimer site which relates to the H bond linearity is bent to 156°.

The 1:2 methanol complex is also found to form a cyclic cluster with the methanol dimer making the link between the OH and CN groups of the chromophore The distances and angles involved in this cluster are very close to those of the 1:2 water complex.

(b) Energies. The total binding energies together with the dissociation energies obtained by subtracting the harmonic zero point energy (Table 3) show that the 1:1 methanol complex is stabilized by about 0.8 kcal/mol relative to the 1:1 water complex. Similarly, D_0 is found to be 1.2 kcal/mol lower in the 1:2 methanol complex relative to the 1:2 water complex. These differences are essentially due to the difference in ZPE energies.

For the 1:2 complexes the two-body contributions (i.e., all components except polarization) have been evaluated by means of the semiempirical method. The $OH_{phenol}\cdots O$ interaction represents the largest contribution (−4.5 and −4.6 kcal/mol for 1:2 water complexes and 1:2 methanol complexes, respectively), while the $OH_{solvent\ donor}\cdots N$ and the solvent−solvent interactions are almost equal (−2.9 kcal/mol). In both complexes, the water and the methanol dimers are squeezed, and the distances and the angles are reduced compared to the "free" dimers. The cooperative effects can be evaluated by the comparison between the sum of the polarization energies of the three molecules and the sum of the polarization energies of the molecules taken two by two. These effects represent 28% and 25% of the total polarization energy for 1:2 water and for 1:2 methanol complexes, respectively.

III. Discussion

Both experimental and calculated data confirm that the observed jet-cooled chromophore is the cis conformer of *o*-cyanophenol. As already mentioned, the OH stretch measured in the IR depletion spectrum is shifted by −72 cm^{-1} with respect to unsubstituted phenol, indicating an interaction between the two substituents associated with the relative orientation of the OH and the cyano groups. The frequency of the same ν(OH) mode has been measured in *o*-fluorophenol by Fujii et al.[8] at 3634 cm^{-1} and is red-shifted by 23 cm^{-1} relative to unsubstituted phenol. This clearly shows that the intramolecular H bond is much stronger in *o*-cyanophenol than in *o*-fluorophenol. The intramolecular OH- -CN interaction confers a chelate structure to the molecule, which is responsible for the dramatic lowering of the S_0-S_1 transition energy as compared to phenol, benzonitrile, or the *p*-cyanophenols.[29]

The computed harmonic normal modes can be used to assign the vibrations active in the dispersed fluorescence spectrum, as shown in Table 1. As mentioned earlier, the calculated frequencies are overestimated relative to the experimentally observed value because of anharmonicity. It is to be noted that the commonly used scaling factor of 0.96 gives a good fit with the experimental results.[38] The most prominent bands observed in dispersed emission can be assigned to in-plane deformations involving the coupling of skeletal motions of the benzene ring with those located on the OH and CN substituents.

A. Structure and IR Spectroscopy of 1:1 Complexes with Water and Methanol. The comparison of experimental results with calculations allows an analysis of the structure of the complexes consistent with the cyclic hydrogen-bonded geometry described before. The three well-separated OH bands observed in the IR spectrum of the water 1:1 complex can be readily attributed according to this structure: at higher frequency a "free" OH (3731 cm^{-1}) band shows up in the water complex spectrum and is absent in the methanol complex and can be correlated to the antisymmetric ν_3 vibration of the H_2O moiety (3756 cm^{-1} in water). On the other hand, the most red-shifted ν(OH) band at 3322 cm^{-1} for the water complex and 3165 cm^{-1} for the methanol complex must be associated with the phenolic OH and exhibits a red shift of respectively 264 and 421 cm^{-1} with respect to bare *o*-cyanophenol. This important shift together with the increasing line width demonstrates a strong OH_{phenol}- - -O hydrogen bond. The remaining bands are found very close in frequency for the water and methanol complexes at 3595 and 3591 cm^{-1}, respectively, and can be correlated with ν_1 of water and ν(OH) of methanol at 3652 and 3681 cm^{-1}. The moderate shift of −57 and −90 cm^{-1} can be easily rationalized by the weak interaction of the solvent OH acting as a hydrogen bond donor toward the CN group of the chromophore. These assignments are well supported by the harmonic normal mode calculations of the cyclic structure, which show that the motions of the bonded OH groups in the bridge are strongly localized, reflecting the difference in the H bond strengths (see Table 4).

The experimental shifts of the $\nu(OH_{phenol})$ stretch induced by complexation can be compared with the calculated ones (Table 4): a good agreement is found for the methanol complex, while the calculated value is overestimated by about 40% for the water complex. If we now take into account the anharmonicity effects, roughly evaluated as mentioned above by calculating the shifts for the deuterated species, the shift obtained in the hydrated complex is correct while it is underestimated for the methanol complex. Moreover, as no difference between the two complexes is observed in their geometry or *De* value, it is difficult to rationalize these results at the level of calculations used here. Indeed, a more sophisticated treatment is required to conclude. First, a frequencies calculation taking into account the anharmonicity effects and obtained at the BSSE-corrected equilibrium geometry has to be performed. Second, potential energy surfaces have to be calculated at a very high level of theory (very large basis set and CCSD(T) method). Unfortunately, these calculations are not tractable because of the complexity of the systems studied here. The calculation of the harmonic frequencies of the "open" structure 1:1 water complex with the *trans-o*-CNPhOH molecule yields three OH stretching vibrations (Table 4). Two of them are very close to the ν_1 and ν_3 bands of the water monomer, indicating that these vibrations are not perturbed by complexation. This behavior is not corroborated by the experimental frequencies. An "open" structure of the 1:1 complexes can be thus firmly ruled out. The difference between the calculated shift of the phenolic OH stretch in the "open" structure 1:1 water complex and the "closed" one is 171 cm^{-1}. This important difference emphasizes the role of the hydrogen-bond water bridge.

Since the interaction between the "open" 1:1 water complex is quite similar to the 1:1 phenol−water[35,36] and phenol−methanol complexes,[39] it is interesting to compare the values of the OH stretch frequencies of these different systems. The calculated shifts of the phenolic OH stretch in the water complex involving the "open" form of *o*-CNPhOH (−274 cm^{-1}) is much larger than that calculated for the phenol−water complex (−118 cm^{-1}).[35] This effect can be related to the stronger acidity of cyanophenols relative to nonsubstituted phenol. We can also consider the frequencies localized on the water molecule: while the frequency reduction of the ν_3 antisymmetric stretching mode of water is of the same order in the "open" complex (calculated −10 cm^{-1}) and in the phenol 1:1 water complex (−7 to −8 cm^{-1}), the symmetric ν_1 stretching mode of water is absent from the water-dimer[37] or phenol−water[40] IR spectrum, because the dipole moment is not changed within the stretching vibration owing to the symmetric structure of the complex. This behavior is confirmed by the very weak calculated intensity of the corresponding vibration in the "open" 1:1 water complex.

The IR calculated intensity of the ν_1 band is one order of magnitude stronger in the "closed" form than in the "open" 1:1 water complex. It appears indeed as a strong band located at 3595 cm^{-1} in the "closed" 1:1 water complex and its width is slightly larger than the experimental resolution (4 cm^{-1}). The intensity of the ν_1 band shows that the two hydrogen atoms of the water molecule do not play a symmetric role in the complex, which is in agreement with the calculated bridge structure in which the water molecule interacts with both OH and CN groups of *o*-cyanophenol.

The comparison of the OH frequency of water and methanol bonded to the CN group (ν_1) obtained in the present work (3595 and 3591 cm^{-1}) with those observed in benzonitrile−water and methanol complexes[41] (3614 and 3624 cm^{-1}) shows that the bridge structure of the *o*-cyanophenol complexes reinforces the OH$_{\mathrm{solvent}}$···CN interaction. For benzonitrile as well as *o*-CNPhOH, the frequency reduction relative to the bare molecule is larger in the methanol complex than in the singly hydrated one. In the benzonitrile complexes, it has been shown that the interaction with water and methanol involves a perpendicular type H-bond to the CN group. Since the hydrogen bond located on the CN group in the *o*-CNPhOH complexes exhibits a similar side-type structure ($C_3-N_4-H_7$ angle of 102°), the decrease in frequencies should be related to the enhancement of the proton-donating character of the water and methanol molecules when bound to the phenol OH.

B. Structure and IR Spectroscopy of the 1:2 Complexes of *o*-Cyanophenol with Water and Methanol. The most stable calculated geometry of the 1:2 complex of *o*-cyanophenol with H_2O exhibits also a cyclic structure in which the water dimer makes a double bridge between the OH$_{\mathrm{phenol}}$ and the CN group. This structure and accompanying harmonic normal modes calculations account for the observed OH stretchs, which exhibit clearly different frequencies and line widths. Among the four IR bands appearing in the 3000−3800 cm^{-1} region, the lowest frequency at 3202 cm^{-1} can be attributed to the phenolic OH and is red shifted by 120 cm^{-1} relative the 1:1 complex. This result together with the broadening of the band shows that the H bond between the chromophore and the solvent is strengthened in agreement with the calculated frequencies and intermolecular distances. In the high-frequency region, normal modes calculations give two close bands separated by 4 cm^{-1} located on the free OH groups (one on each water molecule). Experimentally, however, these two free OH modes are not resolved since only one band is observed at 3722 cm^{-1}. Last, two other bands are found at 3368 and 3573 cm^{-1}. Comparison with the calculated values shows that the highest frequency (3573 cm^{-1}) can be assigned to the OH···CN interaction. This conclusion is corroborated by the fact that similar frequencies due to the OH$_{\mathrm{water}}$···CN or OH$_{\mathrm{methanol}}$···CN were observed in the 1:1 complexes. One can notice here a striking difference between the benzonitrile and *o*-cyanophenol complexes: while the decrease in the water ν(OH) frequency assigned to the OH···CN interaction is larger in *o*-cyanophenol than in benzonitrile for the 1:1 complex, the reverse is observed for the 1:2 complex. When n increases, a change from a "side-type" to a more linear H-bond geometry in benzonitrile:(water)$_n$ has been deduced from the study of ν(CN). Such a transition does not take place in *o*-cyanophenol, owing to the constrained geometry of the complex. The last band is located at 3427 cm^{-1}, and this OH stretch corresponds to the intermolecular H bond within the water dimer. This frequency is, however, much lower than that of the pure water dimer[39] (3601 cm^{-1}). The intermolecular H bond within the water dimer is strongly tightened to adapt between the H bond donor and acceptor sites of *o*-cyanophenol. This result is confirmed by the calculated frequency and structure, which shows that the intradimer O_7-O_9 distance is 2.75 Å compared to 2.98 Å in the free water dimer.[39] The strengthening of the intermolecular bond in the water dimer when embedded in the *o*-cyanophenol molecule reflects the cooperative effects along the hydrogen bonds bridge. The addition of a second water molecule thus enlarges the cyclic structure of the complex and results in the stiffening of the H bond network These remarkable effects have been recently observed in 2-pyridone−(water)$_2$ complexes.[42]

The experimental data on the 1:2 complex with methanol are completely in line with these findings and can be interpreted in a similar way by a dimer of methanol grasped in the jaws of the chromophore substituents: the three observed OH stretching modes can be assigned to the OH$_{\mathrm{phenol}}$ (3065 cm^{-1}), OH$_{\mathrm{methanol\ donor}}$···CN (3505 cm^{-1}) and the intermolecular OH···O of the methanol dimer (3322 cm^{-1}). The reinforcement of the hydrogen-bond network is even stronger than in the water complexes: the intradimer frequency is shifted from 3574[43] to 3322 cm^{-1}, and the chromophore OH donor stretch found at 3085 cm^{-1} is the lowest frequency observed for the systems studied here. As a result of this very large shift, the ν(OH) becomes very close to the phenyl CH vibrations frequencies that appear in the 3000−3100 cm^{-1} range: the vibration is no longer localized on the OH group and couples with the aromatic CH stretch, as shown in the calculations. This coupling explains the breadth of this band and the absence of a well-defined intense feature in this spectral region.[44]

C. Comparison between S_0 and S_1 Properties of the *o*-Cyanophenol and Phenol Complexes.

A common point pertaining to the results of this study is that both the shifts of the S_0-S_1 electronic transition and those of the *o*-cyanophenol OH stretch frequency induced by complexation are large. The UV shifts range from -787 cm^{-1} for the 1:1 complex of water to -1321 cm^{-1} for the 1:2 complex of methanol and are much larger than those obtained in the analogous phenol complexes. A similar trend is observed for the shifts of the ground-state ν(OH) stretch. The cyclic nature of the *o*-cyanophenol complexes may explain these effects since the polarization of the electronic density along the H-bond network should reinforce the accepting character of the solvent. A second important difference relates to the structure of the 1:2 complex with water. In the phenol$-(H_2O)_2$ species it has been found that the phenolic OH acts both as an H bond donor toward one water molecule and as an H bond acceptor from the second water molecule, resulting in a blue shift of the 0$-$0 transition of the 1:2 complex with respect to the 1:1 complex.[44] This is obviously not the case for the *o*-cyanophenol complexes in which the cyclic structure results in a monotonic behavior of the shifts of the electronic transition.

Since the IR frequencies are expected to reflect the strength of the hydrogen bond in the S_0 state and the UV shifts its increase upon excitation, one is tempted to connect both sets of data, as suggested in the case of phenol 1:1 complexes with a series of proton-accepting molecules, for which both the UV and IR shifts correlate with the proton affinity of the solvent.[45] In the case of *o*-CNPhOH, when comparing the two sets of data, it can be seen however that the UV shifts order does not follow that of the IR shifts: while the UV shifts increase smoothly from 1:1 water to 1:1 methanol, 1:2 water, and 1:2 methanol complexes, the order of increasing IR shifts is different (1:1 water, 1:2 water, 1:1 methanol, 1:2 methanol complexes). The reason for this difference is not clear at this point since this behavior is reflected neither in the calculated structure nor in the calculated frequencies. These results emphasize, however, that the magnitude of both UV and IR shifts is not solely linked to the change in the intermolecular H-bond strength but are also a consequence of the H-bonded bridge structure, which may influence them in a different manner. The bridge structure of the complexes is expected to enhance the electronic delocalization upon excitation and thus the red shift of the S_0-S_1 transition. Similarly, the shape of the ground-state potential energy surface that determines the ν(OH) frequency can be very different in the 1:1 and 1:2 complexes because of the constraints imposed by the cyclic structure. In particular, the slope of the repulsion wall must be different, since the H-bond distances are much shorter in the 1:2 complexes than in the 1:1 complexes.

Although the shift of the S_0-S_1 transition is much larger in the case of *o*-cyanophenol complexes than in the phenol complexes, no proton-transfer reaction occurs in the excited state since no fluorescence from the anionic form is detected for any of the complexes under study. A similar behavior (huge red shift with no proton transfer) has been observed in cyclic 1:2 and 1:3 water complexes of 7-hydroxyquinoline.[46,47] This observation is in agreement with a recent theoretical study,[29] which shows that the enhanced acidity of phenol and its cyano derivatives in the S_1 state cannot be attributed to its charge-transfer character but is related to the nature of the lowest electronic state in the conjugated base.

Conclusions

In the present study we have obtained detailed information about intra- and intermolecular H-binding structures in hydrogen-bonded donor$-$acceptor systems by means of double-resonance IR/UV spectroscopy. The theoretical study confirms the experimental results relative to the cyclic structure of the 1:1 and 1:2 *o*-cyanophenol$-$water and $-$methanol complexes. The presence of two neighboring hydrogen bond donor and acceptor sites allows the formation of water and methanol bridges containing one and two solvent molecules. However, it would be interesting to study larger clusters and determine the size at which the transition from a first solvation shell (bridge structure) to a second solvation shell takes place. Furthermore, the formation of a hydrogen-bond network is related to the amphoteric character of the solvent. It is thus expected that nonprotic Lewis bases, whose study is currently in progress, will present different behaviors. Finally, although excited-state proton or hydrogen transfer does not take place in the water and methanol complexes of *o*-cyanophenol, as already found for the phenol and naphthol chromophores, those formed with stronger bases such as amines should be examined in view of exploreing the possibility of inducing the reaction in isolated clusters. Other hydrogen bond donor$-$acceptor systems involving more distant sites such as the *m*-cyanophenol may permit the formation of longer bridges, and these systems would also bring information on the question as to whether the geometric constraints imposed by the interaction between the neighboring OH and CN plays a role in the intermolecular proton transfer.

References and Notes

(1) (a) Syage, J. A. *J. Phys. Chem.* **1995**, *99*, 5772. (b) Douhal, A.; Lahmani, F.; Zewail, A. H. *Chem. Phys.* **1996**, *207*, 477.

(2) Lahmani, F.; Zehnacker-Rentien, A. *J. Phys. Chem.* **1997**, *101*, 6141.

(3) Arnaut, L. G.; Formoshino, S. J. *J. Photochem. Photobiol. A* **1993**, *75*,1.

(4) Tolbert, L. M.; Haubrich, J. E. *J. Am. Chem. Soc.* **1990**, *112*, 8163.

(5) Yamamoto, S.; Ebata, T.; Ito, M. *J. Phys. Chem.* **1989,** *93*, 6340.

(6) Remmers, K.; Meerts, L.; Zehnacker-Rentien, A.; Le Barbu, K.; Lahmani, F. *J. Chem. Phys.* **2000** *112*, 6237.

(7) (a) Bürgi, T.; Leutwyler, S. *J. Chem. Phys.* **1994**, *101*, 8414. (b) Perl, M., G.; Schumm, S.; Henrich, U.; Jacobi, C.; Kleinermanns, K. *J. Chem. Phys.* **1996**, *104*, 9.

(8) Fujii, M.; Iwasaki, A.; Mikami, N. *Chem. Lett.* **1997,** 1099.

(9) Mons, M.; Robertson, E. G.; Snoek, L. D.; Simons, J. P. *Chem. Phys. Lett.* **1999**, *310*, 423.

(10) Frost, R. K.; Hagenmeister, F. C.; Arrington, C. A.; Schleppenbach, D.; Zwier, T. S. *J. Chem. Phys.* **1996**, *105*, 2605.

(11) McMahon, T. B.; Kebarle, P. *J. Am. Chem. Soc.* **1977**, *99*, 2222.

(12) Schulman, S. G.; Vincent W. R.; Underberg W. J. *J. Phys. Chem.* **1981**, *85*, 5, 4068.

(13) Carlson, G. L.; Fateley, W. G. *J. Chem. Phys.* **1973**, *77*, 1157.

(14) Ebata, T.; Fujii, A.; Mikami, N. *Int. Rev. Phys. Chem.* **1998** *331*, 17.

(15) Mani, A.; Hollander, P.; Dreesen, L.; Zheng, W. Q.; Thiry, P.; Tadjedinne, A.; Peremans, A. Manuscript in preparation.

(16) Page, R. H.; Shen, Y. R.; Lee Y. T. *J. Chem. Phys.* **1988**, *88*, 4621.

(17) Riehn, C.; Lahmann, Ch.; Wessermann, B.; Brutschy, B. *Chem. Phys. Lett.* **1997**, *197*, 443.

(18) Tanabe, S.; Ebata, T.; Fujii, M.; Mikami, N. *Chem. Phys. Lett.* **1993,** *215*, 347.

(19) Pribble, R. N.; Zwier, T. S. *Science* **1994,** *265*, 75.

(20) Frisch, M. J.; Trucks, G. W.; Schlegel, H. B.; Scuseria, G. E.; Robb, M. A.; Cheeseman, J. R.; Zakrzewski, W. G.; Montgomery, Jr. J. A.; Stratmann, E.; Burant, J. C.; Dapprich, S.; Millam, J. M.; Daniels, A. D.; Kudin, K. N.; Strain, M. C.; Farkas, O.; Tomasi, J.; Barone, V.; Cossi, M.; Cammi, R.; Mennucci, B.; Pomelli, C.; Adamo, C.; Clifford, S.; Ochterski, J.; Petersson, G. A.; Ayala, P. Y.; Cui, Q.; Morokuma, K.; Malick, D. K.; Rabuck, A. D.; Raghavachari, K.; Foresman, J. B.; Cioslowski, J.; Ortiz, J. V.; Baboul, A. G.; Stefanov, B. B.; Liu, G.; Liashenko, A.; Piskorz, P.; Komaromi, I.; Gomperts, R.; Martin, R. L.; Fox, D. J.; Keith, T.; Al-Laham, M. A.; Peng, C. Y.; Nanayakkara, A.; Challacombe, M.; Gill, P. M. W.; Johnson, B.; Chen, W.; Wong, M. W.; Andres, J. L.; Gonzalez, C.; Head-Gordon, M.; Replogle, E. S.; Pople, J. A. *Gaussian98*, revision A.7; Gaussian, Inc.: Pittsburgh, PA, 1998.

(21) a) Becke, A. D. *J. Chem. Phys.* **1993,** *98*, 5648. (b) Lee, C.; Yang, W.; Parr, R. G. *Phys. Rev. B* **1988**, *37*, 785.

(22) (a) Claverie, P. *Intermolecular Interactions: from diatomics to biopolymers*; Wiley: New York, 1978; Chapter 2. (b) Langlet, J.; Claverie, P.; Boeuvre, F. J. C. *Int. J. Quantum Chem*. **1981**, *19*, 299. (c) Hess, O.; Caffarel, M.; Caillet, J.; Huiszoon, C.; Claverie, P. In *The Proceeding of the 44th international meeting on modeling of molecular structures and properties*; Rivail, J. L., Ed.; Elsevier: Amsterdam, 1990; p 323.

(23) Le Barbu, K.; Brenner, V.; Millié, P.; Lahmani, F.; Zehnacker-Rentien, A. *J. Phys. Chem. A* **1998**, *102*, 128.

(24) (a) Brenner, V.; Millié, P. *Z. Phys. D* **1994**, *30*, 327. (b) Millié, P.; Brenner, V. *J. Chim. Phys. (Paris)* **1995,** *92*, 428

(25) Bockish, F.; Liotard, D.; Rayez, J. C.; Duguay, B. *Int. J. Quantum Chem*. **1992**, *44*, 619.

(26) Metropolis, N.; Rosenbluth, A.; Teller, A.; Teller, E. *J. Chem. Phys.* **1953**, *21*, 1087.

(27) (a) Flether, R. *Comput. J.* **1970**, *13*, 317. (b) Goldfarb, D. *Math. Comput*. **1970**, *24*, 23. (c) Shanno, D. F. *Math. Comput.* **1992**, *24*, 723.

(28) Coussan, S.; Bouteiller, Y.; Perchard, J. P.; Brenner, V.; Millié, Ph.; Zheng, W. Q.; Talbot, F. *J. Chem. Phys.* **1999**, *110***,** 10046.

(29) Granucci, G.; Hynes, J. T.; Millié, P.; Tran Thi, T. *J. Am. Chem. Soc.*, in press.

(30) (a) Dunning, Jr, D. H. *J. Chem. Phys.* **1989**, *90*, 1007. (b) Woon, D. E.; Dunning, T. H., Jr. *J. Chem. Phys.* **1993**, *98*, 1358.

(31) Boys, S. F.; Bernardi, F. *Mol. Phys. B* **1970**, *19*, 553.

(32) Çarçabal, P.; Brenner, V.; Halberstadt, N.; Millié Ph. *Chem. Phys. Lett.* **2000,** *336*, 335.

(33) (a) Latajka, Z.; Bouteiller, Y. *J. Chem. Phys* **1994**, *101*, 9793. (b) Dkhissi, A.; Adamowicz, L.; Maes, G. *Chem. Phys. Lett.* **2000**, *324*, 127.

(34) Duchinsky, F. *Acta Spectrochim. U. R. S. S.* **1937**, *7*, 551.

(35) Schütz, M.; Bürgi, T.; Leutwyler, S. *J. Chem. Phys.* **1992**, *98*, 3763.

(36) Berden, G.; Meerts, L. W.; Schmitt, M.; Kleinermans, K. *J. Chem. Phys.* **1996**, *104*, 972.

(37) Huisken, F.; Kadoulis, M.; Kulke, A. *J. Chem. Phys.* **1996**, *104*, 17.

(38) Palomar, J.; de-Paz, J. L. G.; Catalan, J. *Chem. Phys.* **1999**, *246*, 165.

(39) Schmitt, M.; Küpper, J.; Spangenberg, D.; Westphal, A. *Chem. Phys.* **2000,** *254*, 349.

(40) Watanabe, T.; Ebata, T.; Tanabe, S.; Mikami, N. *J. Chem. Phys.* **1996**, *105*, 408.

(41) Ishikawa, S.; Ebata, T.; Mikami, N. *J. Chem. Phys.* **1999**, *110*, 9504.

(42) Florio, G. M.; Gruenloh, C. J.; Quimpo, R. C.; Zwier, T. S. *J. Chem. Phys.* **2000**, *113*, 11143.

(43) (a) Huisken, F.; Kulcke, A.; Laush, C.; Lisy, J. M. *J. Chem. Phys.* **1991,** *95*, 3924. (b) Huisken, F.; Stemmler, M. *J. Chem. Phys.* **1993**, *98*, 7680.

(44) Oikawa, A.; Abe, H.; Mikami, N.; Ito, M.. *J. Chem. Phys.* **1983**, *87*, 5083.

(45) Iwasaki, A.; Fujii, A.; Watanabe, T.; Ebata, T.; Mikami, N. *J. Phys. Chem.* **1996,** *100*, 16053.

(46) Lahmani, F.; Douhal, A.; Bréhéret, E.; Zehnacker-Rentien, A. *Chem. Phys. Lett.* **1994**, *220*, 235.

(47) Bach, A.; Leutwyler, S. *Chem. Phys. Lett.* **1999,** *299*, 381.